

3-N-2-hydroxyethylamine benzanthrone 및 3-N-2-aminoethylamine benzanthrone에 대한 Cu(II), Ni(II) 및 Co(II) 착물의 분광학, 열 및 생물학적 연구

Moamen S. Refat^{†,‡,*}, Adel S. Megahed^{†,‡}, Ibrahim M. El-Deen[†], Ivo Grabchev[§], and Samir El-Ghol[†]

[†]Department of Chemistry, Faculty of Science, Port Said University, Port Said, Egypt

[‡]Department of Chemistry, Faculty of Science, Taif University, 888-Taif, Kingdom Saudi Arabia

[§]Institute of Polymers, Bulgaria Academy of Science, 1113-Sofia, Bulgaria

(접수 2010. 1. 20; 수정 2010. 10. 8; 게재확정 2010. 12. 6)

Spectroscopic, Thermal and Biological Studies on Newly Synthesized Cu(II), Ni(II) and Co(II) Complexes with 3-N-2-hydroxyethylamine Benzanthrone and 3-N-2-aminoethylamine Benzanthrone

Moamen S. Refat^{†,‡,*}, Adel S. Megahed^{†,‡}, Ibrahim M. El-Deen[†], Ivo Grabchev[§], and Samir El-Ghol[†]

[†]Department of Chemistry, Faculty of Science, Port Said University, Port Said, Egypt. *E-mail: msrefat@yahoo.com

[‡]Department of Chemistry, Faculty of Science, Taif University, 888-Taif, Kingdom Saudi Arabia

[§]Institute of Polymers, Bulgaria Academy of Science, 1113-Sofia, Bulgaria

(Received January 20, 2010; Revised October 8, 2010; Accepted December 6, 2010)

요약. 본 연구에서는 Benzanthrone 치환체인 3-N-2-hydroxy ethylamine benzanthrone (HEAB)와 3-N-2-amino ethylamine benzanthrone (AEAB)의 Cu(II), Co(II) 및 Ni(II) 염화물 착물에 대한 분광학 (IR, UV-vis 및 ¹H-NMR), 원소분석, 몰전도도, 열 무게분석 (TGA/DTG) 및 생물학적 특성에 대해 고찰하였다. 이 연구의 결과에서 HEAB 리간드가 히드록소 및 아미노기를 통하여 각 금속에 배위되어 [Cu(HEAB)(Cl)₂].2H₂O, [Co(HEAB)(Cl)₂(H₂O)₂].8H₂O 및 [Ni(HEAB)(Cl)₂(H₂O)₂].7H₂O 착물을 형성함을 알았다. 한편, AEAB는 [Cu(AEAB)(Cl)₂].2H₂O, [Co(AEAB)(Cl)₂(H₂O)₂].4H₂O 및 [Ni(AEAB)(Cl)₂(H₂O)₂].6H₂O의 분자식을 갖는 팔면체 배위구조를 갖는다. 25 °C DMF에서 모든 착물의 몰전기전도도는 반응안한 리간드보다 약간 컸는데, 이는 염화 이온이 배위권 내부에 존재함을 의미한다. Benzanthrone계 리간드와 이들 착물을 이용하여 서로 다른 종류의 박테리아에 대한 생물활성을 조사하였다.

주제어: Benzanthrone, 전이금속, 착물, 열적 연구, 생물학적 연구

ABSTRACT. Spectroscopic (infrared, electronic and ¹H-NMR), elemental analyses CHN, molar conductivity, thermogravimetric analyses (TGA/DTG) and biological studies, of both benzanthrone derivatives 3-N-2-hydroxy ethylamine benzanthrone (HEAB) and 3-N-2-amino ethylamine benzanthrone (AEAB) with Cu(II), Co(II) and Ni(II) chlorides were discussed herein. Based on the above studies, HEAB ligand was suggested to be coordinated to each metal ions *via* hydroxo and amino groups to form [Cu(HEAB)(Cl)₂].2H₂O, [Co(HEAB)(Cl)₂(H₂O)₂].8H₂O and [Ni(HEAB)(Cl)₂(H₂O)₂].7H₂O coordinated complex. On the other hand, AEAB has an octahedral coordinated feature with formulas [Cu(AEAB)(Cl)₂(H₂O)₂].2H₂O, [Co(AEAB)(Cl)₂(H₂O)₂].4H₂O and [Ni(AEAB)(Cl)₂(H₂O)₂].6H₂O. The molar conductance values at 25 °C for all complexes in DMF are slightly higher than free ligands; this supported the presence of chloride ions inside the coordination sphere. Both benzanthrone ligands and their complexes have been screened against different kinds of bacteria.

Keywords: Benzanthrone, transition metals, complexes, thermal studies, biological studies

INTRODUCTION

Benzanthrone dyes are well known as luminophore dyes emitting in the region from yellow-green to red-purple fluorescence, depending on their structure,¹ their derivatives have a wide variety of applications because of their excellent color characteristics and high photostability.²

Benzanthrone dyes exhibit, both in solution and in the solid state, bright fluorescence and high photostability and find use as dye light fluorescent. Pigments for synthetic textile materials,² due to their bright color, intense fluorescence and good thermostability, are widely used for coloration of polymers.³

Recent studies have shown that at least some benzan-

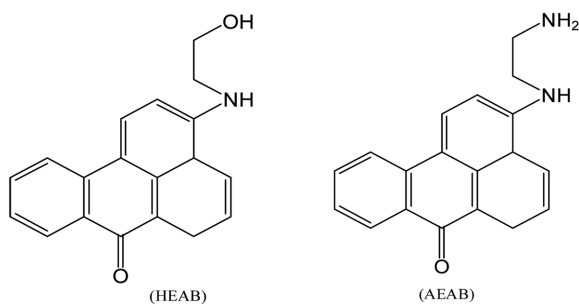


Fig. 1. Structure of benzanthrone derivatives.

throno derivatives have a potential for the nontraditional application as components in color liquid crystalline displays of the “guest-host” type.⁴⁻⁷ Benzanthrone derivatives especially (3-nitrobenzanthrone) are the strongest mutagen,⁸ metabolic activation of nitroaromatic hydrocarbons occurs through N-reduction to form the N-hydroxyl arylamine, which can bind directly to DNA or undergo further activation by esterification to produce species highly reacting with DNA.⁹⁻¹²

On other hand, transition metal complexes play a central role in the construction of molecular materials which display unusual conducting and magnetic properties and find applicability in material chemistry, supramolecules and biochemistry.¹³⁻¹⁷ A number of reviews¹⁸⁻²⁴ have been published on the general biochemistry of copper, electronic aspects of active sites^{25,26} and relevant model chemistry of simple copper complexes,^{27,28} also nickel is one of the most toxic metal among transition metals, it shows the toxicity even in low doses to both plants and animals^{29,30} in general, first row of transition metal complexes with such ligands have a wide range of biological activities.³¹⁻³⁵

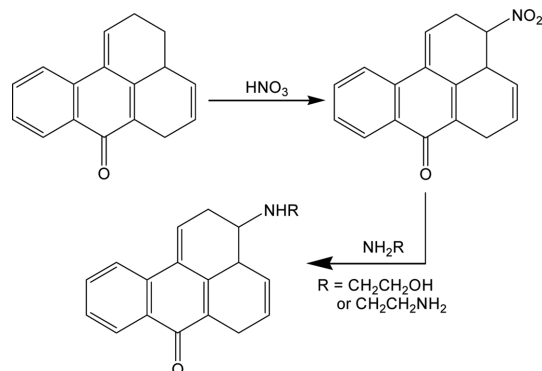
With the great important of benzanthrone and their new transition metal complexes, we are discussed in this paper the spectroscopic characterization, thermal and biological activities. The ligands 3-N-2-hydroxy ethylamine benzanthrone (HEAB) and 3-N-2-amino ethylamine benzanthrone (AEAB) are presented in Fig. 1.

EXPERIMENTAL

$\text{CuCl}_2 \cdot 4\text{H}_2\text{O}$, $\text{CoCl}_2 \cdot 6\text{H}_2\text{O}$ and $\text{NiCl}_2 \cdot 6\text{H}_2\text{O}$ and the other chemicals were purchased from Fluka and Merck companies, and were used without further purification as received.

Synthesis of Ligands

Synthesis of 3-alkyl amino benzanthrone dyes derivatives like (HEAB) and (AEAB) was designed in (Scheme 1). 3-Nitro benzanthrone is the initial product for the syn-



Scheme 1.

thesis of new dyes which was prepared by nitration of benzanthrone.³⁶ The final products were obtained with good yield by nucleophilic substitution of the nitro group in 3-nitro benzanthrone with primary aliphatic amines NH_2R (where $\text{R} = \text{CH}_2\text{CH}_2\text{OH}$; $\text{CH}_2\text{CH}_2\text{NH}_2$) in N,N-dimethylformamide (DMF). In this case, the electron-accepting carbonyl group of the benzanthrone molecule favors the nucleophilic substitution reaction of the nitro group with aliphatic amines NH_2R . The products were characterized by m.p., mass spectra, elemental analysis, IR and $^1\text{H-NMR}$ spectroscopic.

Synthesis of complexes

[Cu(HEAB)(Cl)₂].2H₂O, [Co(HEAB)(Cl)₂(H₂O)₂].8H₂O and [Ni(HEAB)(Cl)₂(H₂O)₂].7H₂O: Each of $\text{CuCl}_2 \cdot 2\text{H}_2\text{O}$ (0.845 g, 0.05 mol), $\text{CoCl}_2 \cdot 6\text{H}_2\text{O}$ (1.19 g, 0.05 mol) or $\text{NiCl}_2 \cdot 6\text{H}_2\text{O}$ (1.19 g, 0.05 mol) was dissolved in ethanol (20 ml) with gently heated. The metal salt solutions were suspended in (10 ml) ethanol of HEAB (2.91 g, 0.1 mol). The reaction mixtures were refluxed for 4 hours at 80 °C. The color complexes were precipitated after cooling, filtered off and washed several times with ethanol and dried under *vacuo* over CaCl_2 .

[Cu(AEAB)(Cl)₂(H₂O)₂].2H₂O, [Co(AEAB)(Cl)₂(H₂O)₂].4H₂O and [Ni(AEAB)(Cl)₂(H₂O)₂].6H₂O: Each of $\text{CuCl}_2 \cdot 2\text{H}_2\text{O}$ (0.845 g, 0.05 mol), $\text{CoCl}_2 \cdot 6\text{H}_2\text{O}$ (1.19 g, 0.05 mol) or $\text{NiCl}_2 \cdot 6\text{H}_2\text{O}$ (1.19 g, 0.05 mol) was dissolved in ethanol (20 ml) with gently heated. The metal salt solutions were suspended in (10 ml) ethanol of AEAB (2.91 g, 0.1 mol). The reaction mixtures were refluxed for 2 hours at 70 °C. The color complexes were precipitated after cooling, filtered off and washed several times with ethanol and dried under *vacuo* over CaCl_2 .

Analysis

Elemental analyses (C, H, and N) were performed using

a Perkin-Elmer CHN 2400 elemental analyzer. The percentage of metal ions was calculated gravimetrically with metal oxides formal. Molar conductance measurements in DMSO solvent at 25 °C for the HEAB and AEAB ligands and their complexes with concentration 1.0×10^{-3} mol/l were carried out using Jenway 4010 conductivity meter. $^1\text{H-NMR}$ spectra were operated using Varian Gemini 200 MHz spectrometer with DMSO as solvent, chemical shift are given in ppm relative to tetramethylsilane. Electron impact mass spectra were recorded on a Jeol, JMS, DX-303 mass spectrometer. The UV/Vis, spectra were obtained in DMSO solution with concentration of (1.0×10^{-3} M) for the (HEAB), (AEAB) ligands and their six complexes with a Jenway 6405 Spectrophotometer using 1 cm quartz cell, in the range of 200-800 nm. Infrared spectra ($4000\text{-}400\text{ cm}^{-1}$) were recorded as KBr pellets on Bruker FT-IR Spectrophotometer.

Thermogravimetric analyses (TG/DTG) were carried out in the temperature range from 25 to 800 °C in a steam of nitrogen atmosphere using Shimadzu TGA 50H thermal analysis. The experimental conditions were: platinum crucible, nitrogen atmosphere with a 30 ml/min flow rate and a heating rate 10 °C/min.

All the antimicrobial experiments involved with the free ligands and their complexes were carried out according to the filter paper disc method. The investigated isolates of bacteria were seeded in tubes with nutrient broth (NB). The seeded NB (1.0 cm^3) was homogenized in the tubes with 9 cm^3 of melted (45 °C) nutrient agar (NA). The

homogeneous suspensions were poured into Petri dishes. The discs of filter paper (diameter 4 mm) were ranged on the cool medium. After cooling on the formed solid medium, 2.0×10^{-5} l of the investigated compounds was applied using a micropipette. After incubation for 24 hours in a thermostat at 25-27 °C, the inhibition (sterile) zone diameters (including disc) were measured and expressed mm. An inhibition zone diameter over 7 mm indicates that the tested compound is active against the bacteria under investigation. The antibacterial activities of the investigated compounds were tested against *Escherichia coli*, *Pseudomonas aeruginosa* as (gram negative), *Bacillus subtilis* and *Staphylococcus aureus* as (gram positive). The concentration of each solution was 1.0×10^{-3} mol/l. Commercial DMSO was employed to dissolve the tested samples.

RESULTS AND DISCUSSION

Satisfactory data of both CHN analysis and the percentage of metals used Cu(II), Co(II) and Ni(II) were confirmed the general formula of the benzanthrone complexes as: $[\text{Cu}(\text{HEAB})(\text{Cl})_2]_2 \cdot 2\text{H}_2\text{O}$; $[\text{M}(\text{HEAB})(\text{Cl})_2(\text{H}_2\text{O})_2] \cdot \text{XH}_2\text{O}$ (where $\text{M}=\text{Co}(\text{II})$ or $\text{Ni}(\text{II})$; $\text{X}=7$ or 8) and $[\text{M}(\text{AEAB})(\text{Cl})_2(\text{H}_2\text{O})_2] \cdot \text{yH}_2\text{O}$, (where $\text{M}=\text{Cu}(\text{II})$; $\text{Co}(\text{II})$ or $\text{Ni}(\text{II})$ and $\text{y}=2$; 4 or 6). The presence of chloride ions in the inner coordination sphere was tested against silver nitrate. The isolated benzanthrone solid complexes have an amorphous powder and structure and stable in air. The analytical and physical properties of the synthetic complexes are given in Table 1.

Table 1. Elemental analysis and physical data of: (A): HEAB, (B): $[\text{Cu}(\text{HEAB})(\text{Cl})_2]_2 \cdot 2\text{H}_2\text{O}$, (C): $[\text{Co}(\text{HEAB})(\text{Cl})_2(\text{H}_2\text{O})_2] \cdot 8\text{H}_2\text{O}$, (D): $[\text{Ni}(\text{HEAB})(\text{Cl})_2(\text{H}_2\text{O})_2] \cdot 7\text{H}_2\text{O}$, (E): AEAB, (F): $[\text{Cu}(\text{AEAB})(\text{Cl})_2(\text{H}_2\text{O})_2] \cdot 2\text{H}_2\text{O}$, (G): $[\text{Co}(\text{AEAB})(\text{Cl})_2(\text{H}_2\text{O})_2] \cdot 4\text{H}_2\text{O}$ and (H): $[\text{Ni}(\text{AEAB})(\text{Cl})_2(\text{H}_2\text{O})_2] \cdot 6\text{H}_2\text{O}$

Compounds	M.Wt	Molar Conductance ($\Omega^{-1}\text{ cm}^2\text{ mol}^{-1}$)	Color	M.P	Yield (%)	Elemental analyses Calc.(found)			
						%C	%H	%N	%M
A	292	9	Black green	216	77%	78.08 (78.72)	6.16 (6.41)	4.49 (4.77)	--
B	462	108	Pink	242	69%	49.35 (49.93)	4.76 (4.52)	3.03 (3.24)	13.63 (14.12)
C	602	92	Brown	>300	66%	37.87 (37.04)	6.31 (6.82)	2.32 (2.56)	9.80 (8.17)
D	584	40	Brown	>300	68%	39.04 (38.61)	6.16 (6.51)	2.39 (2.11)	10.10 (11.23)
E	291	16	Black green	254	78%	78.35 (77.94)	6.52 (6.86)	9.62 (9.29)	---
F	497	44	Brown	>300	76%	45.87 (44.01)	5.43 (5.92)	5.63 (6.01)	12.67 (11.22)
G	528	92	Pink	>300	68%	43.10 (42.50)	5.86 (5.13)	5.29 (5.45)	11.15 (12.67)
H	565	38	Pink	>300	65%	40.35 (40.80)	6.19 (6.04)	4.95 (5.10)	10.44 (9.85)

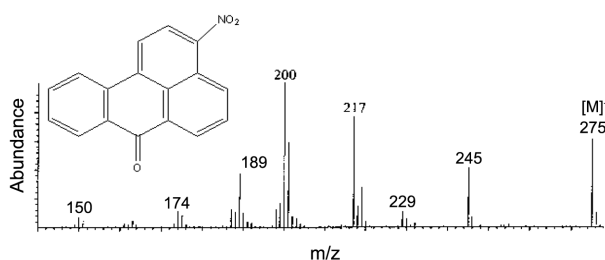


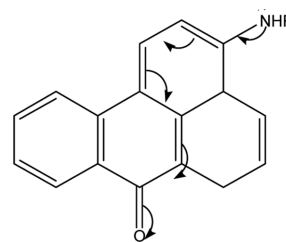
Fig. 2. Electron impact mass spectra of 3-nitrobenzanthrone.

Mass Spectra

The electron impact mass spectrum of the start material 3-nitrobenzanthrone show the following molecular ions and characteristic fragment ions (Fig. 2). Molecular ion at 275 m/z and base peak at 200 m/z and the other fragments appeared at 150, 174, 189, 217, 229 and 245.

Molar conductance

The molar conductance (Λ_m) values of benzanthrone and their metal(II) complexes (Table 1) have been performed using DMSO as solvent at 25 °C with concentration of 10^{-3} M. The molar conductance of these complexes lies in the range of 39-108 $\Omega^{-1}\text{cm}^2\text{mol}^{-1}$. These results indicate that the behavior of these complexes is a slightly electrolytic nature comparison with free ligand. According to the mentioned results, we can deduce that the chloride ions were appeared inside the coordination sphere of all complexes and the difference range of molar conductance depends upon the degree of the soluble of each complex. The molar conductance data was agreement with the proposed composition of formed complexes.



Scheme 2.

Electronic Spectra

The electron donor-acceptor interaction with 3-substituted benzanthrone occurs between its electron-accepting (carbonyl group) and the electron-donating group in C-3 position of the chromophoric system,³⁶ the path of the charge-transfer is given on Scheme 2. The spectra of the ligand 3-N-2-hydroxy ethylamine benzanthrone (HEAB) in DMF are shown in Fig. 3. There are two detected absorption bands at around 233 and 362 nm assigned to $\pi-\pi^*$ and $n-\pi^*$, respectively, intraligand transitions. These transitions also found in the spectra of the complexes but they are shifted and increased in the intensity confirming the coordination of the ligand to the metal ions Table 2. The spectra of the ligand 3-N-2-amino ethylamine benzanthrone (AEAB) in DMF are shown in Fig. 3. There are two detected absorption bands at around 232 and 387 nm Table 2. Assigned to $\pi-\pi^*$ and $n-\pi^*$, respectively, the 3-substituted benzanthrone derivatives exhibited the following disposition of the energetic levels $T\pi-\pi^* < S\pi-\pi^* < Tn-\pi^* < Sn-\pi^*$.^{37,38}

Spectroscopic characterization

Infrared Spectrum: Table 3 includes the most important IR spectral data of 3-N-2-hydroxy ethylamine ben-

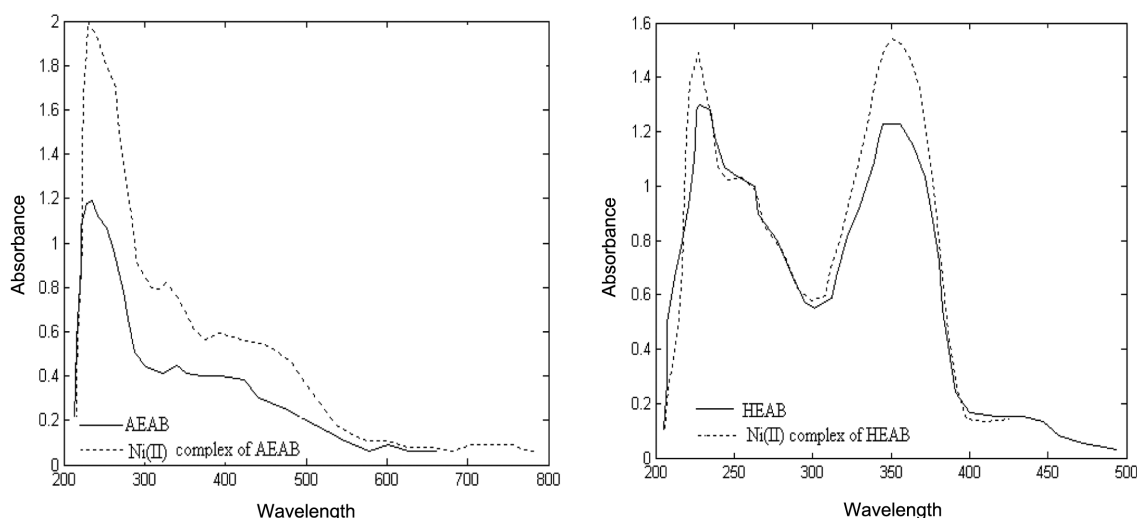


Fig. 3. Electronic spectra of HEAB, AEAB and its nickel complexes.

Table 2. Electronic spectra of HEAB, AEAB and their complexes

Compounds	λ_{max} (nm)	ϵ ($\text{mol}^{-1} \text{cm}^{-1}$)	Assignment
HEAB	233, 362	1400, 1350	$\pi - \pi^*$, $n - \pi^*$
$\text{Cu(HEAB)(Cl)}_2 \cdot 2\text{H}_2\text{O}$	235, 362	1510, 1517	$\pi - \pi^*$, $n - \pi^*$
$[\text{Co(HEAB)(Cl)}_2(\text{H}_2\text{O})_2] \cdot 8\text{H}_2\text{O}$	235, 365	1592, 1498	$\pi - \pi^*$, $n - \pi^*$
$[\text{Ni(HEAB)(Cl)}_2(\text{H}_2\text{O})_2] \cdot 7\text{H}_2\text{O}$	237, 366	1492, 1487	$\pi - \pi^*$, $n - \pi^*$
AEAB	232, 287	1223, 481	$\pi - \pi^*$, $n - \pi^*$
$[\text{Cu(AEAB)(Cl)}_2(\text{H}_2\text{O})_2] \cdot 2\text{H}_2\text{O}$	235, 390	2631, 810	$\pi - \pi^*$, $n - \pi^*$
$[\text{Co(AEAB)(Cl)}_2(\text{H}_2\text{O})_2] \cdot 4\text{H}_2\text{O}$	236, 391	1974, 523	$\pi - \pi^*$, $n - \pi^*$
$[\text{Ni(AEAB)(Cl)}_2(\text{H}_2\text{O})_2] \cdot 6\text{H}_2\text{O}$	236, 391	1955, 557	$\pi - \pi^*$, $n - \pi^*$

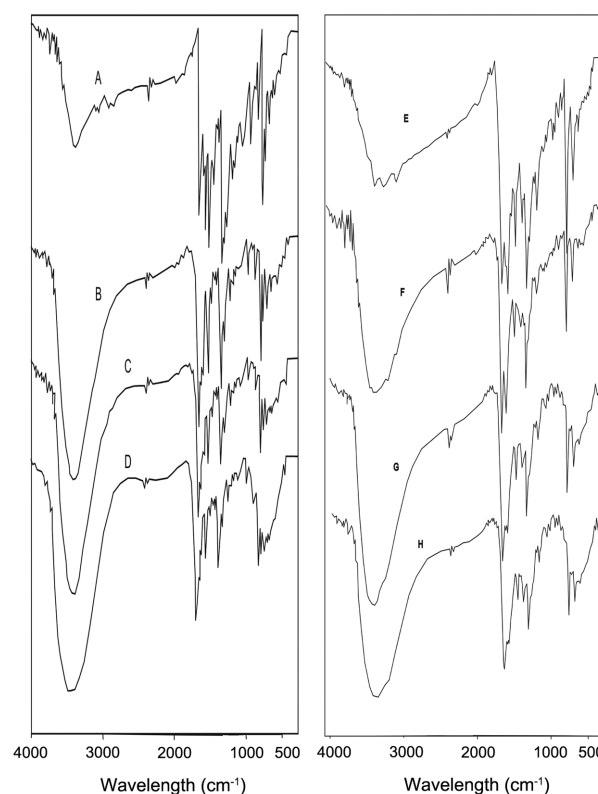
Table 3. Infrared spectra of: (A): HEAB, (B): $[\text{Cu(HEAB)(Cl)}_2] \cdot 2\text{H}_2\text{O}$, (C): $[\text{Co(HEAB)(Cl)}_2(\text{H}_2\text{O})_2] \cdot 8\text{H}_2\text{O}$, (D): $[\text{Ni(HEAB)(Cl)}_2(\text{H}_2\text{O})_2] \cdot 7\text{H}_2\text{O}$, (E): AEAB, (F): $[\text{Cu(AEAB)(Cl)}_2(\text{H}_2\text{O})_2] \cdot 2\text{H}_2\text{O}$, (G): $[\text{Co(AEAB)(Cl)}_2(\text{H}_2\text{O})_2] \cdot 4\text{H}_2\text{O}$ and (H): $[\text{Ni(AEAB)(Cl)}_2(\text{H}_2\text{O})_2] \cdot 6\text{H}_2\text{O}$

Compounds	$\nu(\text{OH})$ hydrated	$\nu(\text{OH})$ Coord.	$\nu(\text{C}=\text{O})$	$\nu(\text{OH})$	$\nu(\text{N}-\text{H})$	$\nu(\text{NH}_2)$	$\nu(\text{M}-\text{N})$	$\nu(\text{M}-\text{O})$
A	--	--	1662 (s)	3386(br)	3066(m)	--	--	--
B	3440(br)	848(m)	1652 (s)	3362(br)	3052(m)	--	550(w)	421(w)
C	3444(br)	846(m)	1651 (s)	3367(br)	3047(m)	--	544(w)	416(w)
D	3442(br)	847(m)	1651 (s)	3366(br)	3049(m)	--	550(w)	418(w)
E	--	--	1641 (s)	--	3062(m)	3350(br)	--	--
F	3431(br)	878(m)	1649 (s)	--	3039(m)	3331(br)	550(w)	427(w)
G	3433(br)	878(m)	1638 (s)	--	3040(m)	3337(br)	542(w)	424(w)
H	3430(br)	878(m)	1638 (s)	--	3041(m)	3335(br)	530(w)	420(w)

zanthrone (HEAB) and 3-N-2-amino ethylamine benzanthrone (AEAB) and their metal complexes. Infrared spectra of the ligand (HEAB), showed two absorption broad bands in the region of 3386 and 3202 cm^{-1} , which assigned to the stretching vibrations of $\nu(\text{O}-\text{H})$ and secondary amino group $\nu(\text{N}-\text{H})$, respectively. The band at 1175 cm^{-1} assigned to stretching vibration $\nu(\text{C}-\text{N})$ (imide band) and the absorption band at 1059 cm^{-1} assigned to stretching vibration $\nu(\text{C}-\text{O})$. On complexation the position of these bands are shifted toward higher wave number by 8-19 cm^{-1} and 12-18 cm^{-1} , respectively, (Fig. 4).

On the other hand, ligand (AEAB) contain amino group (NH_2) and secondary amino group $\nu(\text{NH})$ showed absorption broad bands in the region of 3350 cm^{-1} and 3231 cm^{-1} , which can be assigned to stretching vibrations $\nu(\text{NH}_2)$ and secondary amino group $\nu(\text{NH})$, respectively. The band at 1085 cm^{-1} and 1174 cm^{-1} assigned to stretching vibration $\nu(\text{C}-\text{N})$ of NH_2 and $\nu(\text{C}-\text{N})$ of NH , respectively. After complex formation the position of stretching vibrations of (NH_2) and secondary amino group (NH) are shifted toward higher wavenumber by 10-17 cm^{-1} and 14-18 cm^{-1} , respectively. The band of stretching vibration $\nu(\text{C}-\text{N})$ of (NH_2) and stretching vibration $\nu(\text{C}-\text{N})$ of (NH) are shifted toward lower wavenumber by $\sim 17 \text{cm}^{-1}$ and $\sim 5 \text{cm}^{-1}$, respectively.

Infrared spectra of complexes exhibited broad bands at 3430-3440 cm^{-1} that are attributed to $\nu(\text{OH})$ of the crystal water molecules. While the bands observed at approxi-

**Fig. 4.** Infrared spectra of: A=HEAB; B= $[\text{Cu(HEAB)(Cl)}_2] \cdot 2\text{H}_2\text{O}$; C= $[\text{Co(HEAB)(Cl)}_2(\text{H}_2\text{O})_2] \cdot 8\text{H}_2\text{O}$; D= $[\text{Ni(HEAB)(Cl)}_2(\text{H}_2\text{O})_2] \cdot 7\text{H}_2\text{O}$ E=AEAB; F= $[\text{Cu(AEAB)(Cl)}_2(\text{H}_2\text{O})_2] \cdot 2\text{H}_2\text{O}$; G= $[\text{Co(AEAB)(Cl)}_2(\text{H}_2\text{O})_2] \cdot 4\text{H}_2\text{O}$; H= $[\text{Ni(AEAB)(Cl)}_2(\text{H}_2\text{O})_2] \cdot 6\text{H}_2\text{O}$.

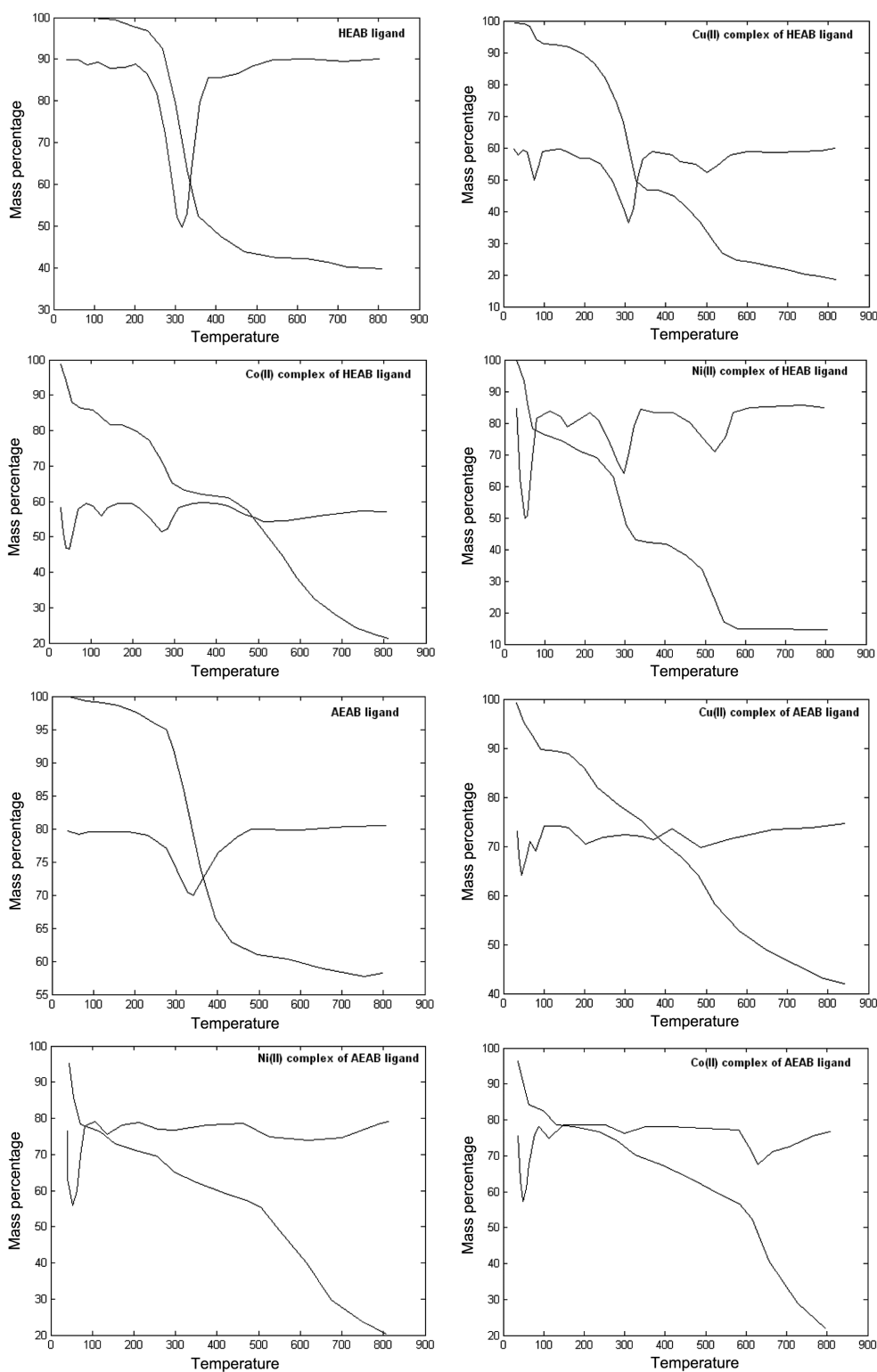


Fig. 5. TGA diagrams of HEAB, AEAB ligands and their metal complexes.

mately 878 cm^{-1} are assigned to coordinated water molecules.³⁹ Bands in the region ~ 550 and ~ 420 may be assigned

to $\nu(\text{M-N})$ and $\nu(\text{M-O})$, respectively.⁴⁰ This result indicates that the coordination takes place through the nitro-

gen and oxygen atoms of NH and OH groups in 3-N-2-hydroxy ethylamine benzanthrone (HEAB) and through both of nitrogen atoms of NH₂ and NH groups in 3-N-2-amino ethylamine benzanthrone (AEAB) Fig. 4.

¹H-NMR Spectrum: The chemical shift (δ , ppm) of the proton magnetic resonance of both HEAB and AEAB have been recorded as follows:

¹HNMR (DMSO-d₆ at 200MHZ):

(HEAB): δ : 2.43(s,1-H):OH; 3.54(t,2H):NCH₂; 3.72(t,2H):OCH₂; 4.16(s, 1-H): NH; 6.66(d,1H,J=8.0 HZ):2-H; 7.26(m,1H): 5-H, 8-H and 10-H; 7.80(m, 2H): 4-H and 9-H; 8.24(m, 2H): 6-H and 7-H: 8.56(d, 1H, J=8.0 HZ): 1-H.⁴¹

(AEAB): δ =2.54(t,2-H):NH₂; 3.42(t,2H)NCH₂; 3.30(t,2H):(NH₂)CH₂; 3.40(s, 1-H): NH; 6.89(d,1H,J=8.0 HZ): 2-H; 7.85(m,1H): 5-H, 8-H and 10-H; 8.17(m, 2H): 4-H and 9-H; 8.40(m, 2H): 6-H and 7-H: 8.62(d, 1H, J=8.0 HZ): 1-H.

Thermal Studies

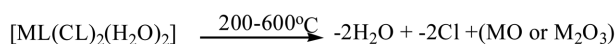
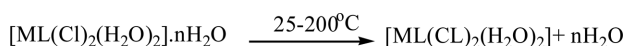
The thermal degradation of all complexes was studied using thermogravimetric techniques and a temperature range of 25-800 °C (Fig. 5). The thermal stability data are listed

in Table 4. The data from thermogravimetric analysis clearly indicated that the decomposition of the complexes proceeds in three or four steps. Crystal water molecules were lost in between 25-150 °C and chloride ions or coordinated water molecules were lost in between 200-350 °C. Metal oxides were formed above 600 °C for the Cu(II), Co(II) and Ni(II) complexes. The thermal analysis of ligands 3-N-2-hydroxy ethylamine benzanthrone (HEAB) and 3-N-2-amino ethylamine benzanthrone (AEAB) melts at 216 and 254 °C, respectively, with simultaneous decomposition. The main degradation peaks were observed at 314 and 334 °C in the TG profile. From the TG profile of (HEAB) and (AEAB), it appears that the sample decomposes in one sharp stage over the wide temperature range 25-800 °C. The decomposition occurs with a mass loss of 62.81% and its calculated value is 63.01% for (HEAB) ligand and mass loss of 47.23% and its calculated value is 46.70% for (AEAB) ligand.

The thermal analysis of the chelates under study evinces the following weight losses 7.11-20.89% loss of water molecules of hydration over the rang 25-120 °C interval

Table 4. Thermo gravimetric data of: (A): HEAB, (B): [Cu(HEAB)(Cl)₂].2H₂O, (C): [Co(HEAB)(Cl)₂(H₂O)₂].8H₂O, (D): [Ni(HEAB)(Cl)₂(H₂O)₂]. 7H₂O, (E): AEAB, (F): [Cu(AEAB)(Cl)₂(H₂O)₂].2H₂O, (G): [Co(AEAB)(Cl)₂(H₂O)₂].4H₂O and (H): [Ni(AEAB)(Cl)₂(H₂O)₂].6H₂O

Complexes	Steps	Temperature rang(°C)	DTG peak (°C)	TG Weight loss % calc./found	Assignments
A	1 st	25-800 800-	314	63.01(62.81) 36.98(37.19)	C ₁₀ H ₁₈ NO ₂ 9C
B	1 st	25-120	77	7.79(7.77)	2H ₂ O
	2 nd	120-350	302	49.56(48.74)	2Cl + C ₁₀ H ₈ NO
	3 rd	350-600 600-	501	20.38(21.21) 22.27(22.28)	C ₇ H ₁₀ CuO + 2C
C	1 st	25-120	60	17.94(16.65)	6H ₂ O
	2 nd	120-200	126	5.98(6.10)	2H ₂ O
	3 rd	200-300	273	17.77(18.37)	2Cl+2H ₂ O
	4 th	300-600 600-	556	33.22(32.61) 25.08(26.27)	C ₁₄ H ₁₈ N 1/2(Co ₂ O ₃)+1/2O ₂ +5C
D	1 st	25-120	55	21.56(20.89)	7H ₂ O
	2 nd	120-200	150	6.16(6.58)	2H ₂ O
	3 rd	200-360	295	28.25(29.00)	2Cl+C ₅ H ₄ NO
	4 th	360-600 600-	523	27.05(27.49) 16.95(16.04)	C ₁₂ H ₁₄ NiO + 2C
E	1 st	25-400 400-	334	46.7(47.23) 53.3(52.77)	C ₆ H ₁₉ N ₂ O 13C
F	1 st	25-120	80	7.24(7.11)	2H ₂ O
	2 nd	120-380	150	21.52(22.81)	2Cl+2H ₂ O
	3 rd	380-600 600-	317	43.25(42.43) 27.94(27.67)	C ₁₄ H ₁₉ N ₂ CuO + 5C
G	1 st	25-120	70	13.60(13.88)	4H ₂ O
	2 nd	120-200	115	3.40(3.10)	H ₂ O
	3 rd	200-650 650-	625	58.98(57.64) 24.02(25.38)	2Cl+C ₁₆ H ₂₁ N ₂ 1/2(Co ₂ O ₃)+1/2O ₂ +3C
H	1 st	25-120	80	19.08(20.11)	6H ₂ O
	2 nd	120-200	150	6.36(7.01)	2H ₂ O
	3 rd	200-600 600-	500	52.74(51.17) 21.75(21.71)	2Cl + C ₁₅ H ₁₉ N ₂ NiO + 4C



where MO = CuO, NiO; M₂O₃ = Co₂O₃; n = 1-8

Scheme 3. The thermal decomposition stages of benzanthrone complexes.

(calculated 7.24-21.56%) for the Cu(II), Co(II) and Ni(II) complexes.

- 3.10-7.01% loss of water molecules of coordination over the range 120-360 °C interval (calculated 3.40-6.36%) for Co(II) and Ni(II) complexes.
- 27.28-48.745 elimination of Cl₂ molecules and organic moiety over the range 120-380 °C interval (calculated 21.52-49.56%) for Cu(II) complexes.
- 18.37-57.64% elimination of Cl₂ molecules and organic moiety over the temperature range 200-600 °C interval (calculated 17.77-58.98%) for the Co(II) and Ni(II) complexes.
- 16.04-27.67% residues of metal oxides remain over 600-800 °C interval (calculated 16.95-27.94%) for Cu(II), Co(II) and Ni(II) complexes.

In general, the stages of thermal decomposition of the complexes can be written as *Scheme 3*.

Kinetic studies

In recent years, there has been increasing interest in determining the rate-dependent parameters of solid-state non-isothermal decomposition reactions by analysis of

TG curves. Several equations⁴²⁻⁴⁹ have been proposed as means of analyzing a TG curve and obtaining values for kinetic parameters. Many authors⁴²⁻⁴⁶ have discussed the advantages of this method over the conventional isothermal method.

Most commonly used methods for this purpose are the differential method of Freeman and Carroll⁴² integral method of Coat and Redfern,⁴⁴ the approximation method of Horowitz and Metzger.⁴⁷ In the present investigation, the general thermal behaviors of the complexes in terms of stability ranges, peak temperatures and values of kinetic parameters are listed in *Table 5*. The kinetic parameters have been evaluated using the mentioned methods and the results obtained by these methods are well agreement with each other.

The entropy of activation, ΔS^* , enthalpy activation, ΔH^* , and Gibbs free energy, ΔG^* , were calculated from; $\Delta H^* = E^* - RT$ and $\Delta G^* = \Delta H^* - T\Delta S^*$, respectively.

From the kinetic and thermodynamic data resulted from the TGA curves and tabulated in *Table 5*, the following outcome can be discussed as follows:

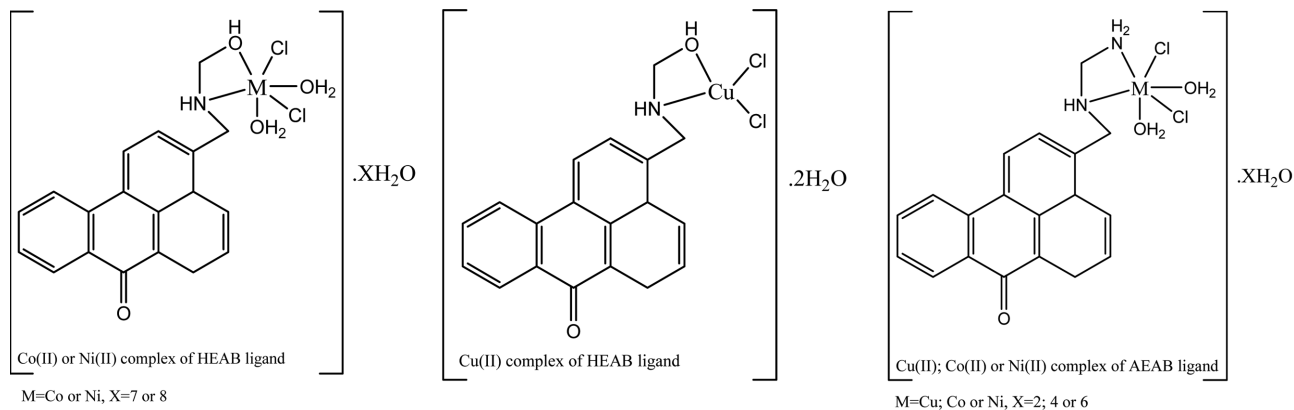
1. The thermodynamic data obtained with the two methods are in harmony with each other.
2. The higher values of activation energies of the both HEAB and AEAB benzanthrone complexes led to thermal stability of the studied complexes.
3. The activation energy of Cu⁺² and Ni⁺² complexes is expected to increase in relation with decrease in their radii. The smaller size of the ions permits a closer approach of the ligand. Hence, the E value in the first

Table 5. Kinetic Parameters using the Coats-Redfern (CR) and Horowitz-Metzger (HM) for: (A): HEAB, (B): [Cu(HEAB)(Cl)₂].2H₂O, (C): [Co(HEAB)(Cl)₂(H₂O)₂].8H₂O, (D): [Ni(HEAB)(Cl)₂(H₂O)₂].7H₂O, (E): AEAB, (F): [Cu(AEAB)(Cl)₂(H₂O)₂].2H₂O, (G): [Co(AEAB)(Cl)₂(H₂O)₂].4H₂O and (H): [Ni(AEAB)(Cl)₂(H₂O)₂].6H₂O

Complex	Stage	Method	Parameters					r
			E (J mol ⁻¹)	A (s ⁻¹)	ΔS (J mol ⁻¹ K ⁻¹)	ΔH (J mol ⁻¹)	ΔG (J mol ⁻¹)	
A	2 nd	CR	8.09 × 10 ⁴	8.35 × 10 ⁴	-156	7.60 × 10 ⁴	1.68 × 10 ⁵	0.99766
		HM	9.37 × 10 ⁴	1.78 × 10 ⁶	-131	8.89 × 10 ⁴	1.61 × 10 ⁵	0.99783
B	2 nd	CR	1.05 × 10 ⁵	3.10 × 10 ⁷	-107	1.01 × 10 ⁵	1.66 × 10 ⁵	0.99592
		HM	1.15 × 10 ⁵	3.13 × 10 ⁸	-87.7	1.11 × 10 ⁵	1.62 × 10 ⁵	0.99976
C	2 nd	CR	9.29 × 10 ⁴	6.07 × 10 ⁶	-120	8.83 × 10 ⁴	1.54 × 10 ⁵	0.98983
		HM	9.96 × 10 ⁴	3.38 × 10 ⁷	-106	9.51 × 10 ⁵	1.53 × 10 ⁵	0.99707
D	2 nd	CR	1.15 × 10 ⁵	4.60 × 10 ⁸	-84.4	1.11 × 10 ⁵	1.59 × 10 ⁵	0.99775
		HM	1.27 × 10 ⁵	5.71 × 10 ⁹	-63.5	1.22 × 10 ⁵	1.59 × 10 ⁵	0.9999
E	2 nd	CR	8.78 × 10 ⁴	3.50 × 10 ⁸	-87.3	8.28 × 10 ⁴	1.36 × 10 ⁵	0.99874
		HM	8.65 × 10 ⁴	1.94 × 10 ⁵	-150	8.14 × 10 ⁴	1.72 × 10 ⁵	0.99892
F	2 nd	CR	0.92 × 10 ⁵	3.96 × 10 ⁵	-144	8.69 × 10 ⁴	1.77 × 10 ⁵	0.99528
		HM	1.01 × 10 ⁵	2.28 × 10 ⁶	-129	9.63 × 10 ⁴	1.77 × 10 ⁵	0.99512
G	2 nd	CR	4.60 × 10 ⁴	5.81 × 10 ⁴	-160	4.08 × 10 ⁴	1.41 × 10 ⁵	0.99178
		HM	6.36 × 10 ⁴	9.56 × 10 ²	-194	5.84 × 10 ⁴	1.80 × 10 ⁵	0.97988
H	2 nd	CR	6.61 × 10 ⁴	8.18 × 10 ³	-175	6.16 × 10 ⁴	1.57 × 10 ⁵	0.99367
		HM	7.24 × 10 ⁴	6.31 × 10 ⁴	-158	6.79 × 10 ⁴	1.54 × 10 ⁵	0.99821

Table 6. Antibacterial activity data of the benzanthrone ligands and their metal complexes, inhibition zone(mm)

Compound	Bacillus subtili G ⁺	Staphylococcus aureus G ⁺	Escherichia coli G ⁻	Pseudomonas aeruginosa G ⁻
HAEB	18	19	18	20
[Cu(HEAB)Cl ₂].2H ₂ O	15	16	16	17
[Co(HEAB)(Cl) ₂ (H ₂ O) ₂].8H ₂ O	18	20	20	18
[Ni(HEAB)(Cl) ₂ (H ₂ O) ₂].7H ₂ O	18	19	18	18
AEAB	18	19	18	20
[Cu(AEAB)(Cl) ₂ (H ₂ O) ₂].2H ₂ O	15	13	16	16
[Co(AEAB)(Cl) ₂ (H ₂ O) ₂].4H ₂ O	20	15	22	20
[Ni(AEAB)(Cl) ₂ (H ₂ O) ₂].6H ₂ O	18	14	20	20

**Fig. 6.** Suggested structures of the Cu(II), Co(II) and Ni(II) benzanthrone complexes.

stage for the Ni²⁺ complex is higher than that for the other Cu⁺² and Co⁺² complexes.

- The correlation coefficients of the Arrhenius plots of the thermal decomposition steps were found to lie in the range 0.9820 to 0.9996, showing a good fit with linear function.

It is clear that the thermal decomposition process of all benzanthrone complexes is non-spontaneous, i.e., the complexes are thermally stable.

Microbiological investigation

The results of antibacterial actives in vitro of the ligand and all their complexes are represented in Table 6. From the results we can see that all the test compounds have a high activity as antibacterial against gram positive (*Bacillus subtili*, *staphylococcus aureus*) and also toward gram negative (*Escherichia coli*, *Pseudomonas aeruginosa*).

The sequence of the antibacterial activity of the Cu(II), Co(II) and Ni(II) benzanthrone complexes can be designed as follows according to the kind of bacteria:

i. *Bacillus subtili*: Co/AEAB>HEAB=Co/HEAB=Ni/HEAB=AEAB=Ni/AEAB>Cu/HEAB=Cu/AEAB

ii. *staphylococcus aureus*: Co/HEAB>HEAB=Ni/HEAB=AEAB>Cu/HEAB>Co/AEAB>Ni/AEAB>Cu/AEAB

iii. *Escherichia coli*: Co/AEAB>Co/HEAB=Ni/AEAB>HEAB=Ni/HEAB=AEAB>Cu/HEAB=Cu/AEAB

iv. *Pseudomonas aeruginosa*: HEAB=AEAB=Co/AEAB=Ni/AEAB>Co/HEAB=Ni/HEAB>Cu/HEAB>Cu/AEAB

Generally, The Co(II) benzanthrone complexes have a higher antibacterial activity than other Cu(II) and Co(II) benzanthrone complexes.

Structure of the benzanthrone complexes

Finally on the basis of the above studies; the suggested structures of the Cu(II), Co(II) and Ni(II) benzanthrone complexes can be represented in Fig. 6.

CONCLUSION

In conclusion, we have synthesized and characterized six mononuclear Cu(II), Co(II) and Ni(II) complexes of both benzanthrone derivatives 3-N-2-hydroxy ethylamine benzanthrone (HEAB) and 3-N-2-amino ethylamine benzanthrone (AEAB). The complexes have been screened for antibacterial activity against four bacteria. All complexes were discussed using infrared, electronic, ¹H-NMR, elemental analyses CHN, molar conductivity and thermogravimetric TGA/DTG investigations.

REFERENCE

- Carlini, F.; Paffoni, C.; Bpffa, G. *Dyes and Pigments*

- 1982, 3, 59.
2. Krasovitski, B.; Bolotin, B. *Organic luminophore*; Chimia: leningrade, 1984 (in Russian).
 3. Konstantinova, T. N.; Lazarova, R. A. *Dyes and Pigments* **2007**, 74, 208.
 4. Grabchev, I.; Monevai, I. *Comp. Rend. Acad. Bulg. Sci.* **1997**, 50(6), 59.
 5. Grabchev, I.; Bojinov, V.; Moneva, I. *J. Mol. Str.* **1998**, 19, 271.
 6. Grabchev, I.; Moneva, I. *Dyes and Pigments* **1998**, 37, 155.
 7. Grabchev, I.; Bojinov, V.; Moneva, I. *Dyes and Pigments* **2001**, 48, 143.
 8. Enya, T.; Suzuki, H.; Hirayama, T.; Hisamatsu, Y. *Environ. Sci. Technol.* **1997**, 31, 2772.
 9. Beland, F. A.; Kadlubar, F. F. *Handbook of experimental pharmacology Chemical Carcinogenesis and Mutagenesis*; Springer: Heidelberg, **1990**, 94(1), 267-325.
 10. Beland, F. A.; Marrques, M. M. *International Agency for Research on cancer*; Lyon: France, 1994; pp 229-244.
 11. Hanna, P. E.; Banks, R. B. *Arylhydroxylamines and arylhydroxamic acids: conjugation reactions*; Anders, M. W., Ed.; *Bioactivation of foreign compounds*; Academic Press: Orlando, Fla, 1985; pp 375-402.
 12. Kadlubar, F. F.; Beland, F. A., *Chemical properties of ultimate carcinogenic metabolites of arylamines and arylamides. In: Polycyclic Hydrocarbons and Carcinogenesis*; American Chemical Society: Washington, DC, 1985, pp 341-370.
 13. Solomon, E. I.; Brunold, T. C.; Davis, M. Z.; Kemsley, J. N.; Lee, S. K.; Lehnert, N.; Skulan, A. J.; Yang, Y. S.; Zhou, J. *Chem. Rev.* **2000**, 100, 253.
 14. Chandra, S.; Kumar, R. *Trans. Met. Chem.* **2003**, 29(3), 269.
 15. Chandra, S.; Kumar, R. *Spectrochim. Acta part A* **2005**, 61, 437.
 16. Chandra, S.; Kumar, R. *Synth. React. Inorg. Met. Org. Nano-Met. Chem.* **2005**, 35, 103.
 17. Spirro, T. G. *Metal Ion in Biology*; Wiley: NY, Vol. 13, 1981.
 18. Sigel, H. *Metal Ion in Biology Systems*; Dekker: NY, Vol. 13, 1981.
 19. Fee, J. A. *Struct. Bond. (Berl.)* **1975**, 1, 23.
 20. CIBA Foundation Symposium no. 79, Excerpt, Medica, Amsterdam, 1980.
 21. Beinert, H. *Coord. Chem. Rev.* **1980**, 279, 33.
 22. Reinhammer, B. *Adv. Inorg. Biochem.* **1979**, 91, 1.
 23. Laurie, S. H.; Mohammed, E. S. *Coord. Chem. Rev.* **1980**, 279, 33.
 24. Soloman, E. I.; Penfield, K. W.; Wilcox, D. E. *Struct. Bond (Berl.)* **1983**, 1, 53.
 25. Gray, H. B.; Soloman, E. I.; Spiro, T. G. *Metal Ions in Biology*; Wiley: NY, 1981, p 3.
 26. Sigel, H. *Metal Ions in Biological Systems*; Dekker: NY, Vol. 12, 1980.
 27. Ulrich, E.; Markley, J. L. *Coord. Chem. Rev.* **1978**, 109, 27.
 28. Swearingen, J. K.; West, D. X. *Trans. Met. Chem.* **2001**, 26, 252.
 29. Wood, J. M.; Sigel, H. *Microbial Strategies in Resistance to Metal Ion Toxicity Metal Ion in Biology*; Marcel Dekker: York, 1984.
 30. Joud, E. M.; Riou, A.; Allian, M.; Khan, M. A.; Bouet, G. M. *Polyhedron* **2001**, 20, 67.
 31. Xinde, Z.; Wang, C.; Lu, Z.; Dang, Y. *Trans. Met. Chem.* **1997**, 22, 13.
 32. Chandra, S.; Gupta, K. *Trans. Met. Chem.* **2002**, 27, 196.
 33. Dhiman, A. M.; Wododker, K. N. *Indian J. Chem.* **2001**, B40, 636.
 34. Chandra, S.; Gupta, K. *Trans. Met. Chem.* **2002**, 27, 329.
 35. Shioda, H.; Kato, S.; *Juki Kagakaishi* **1957**, 15, 362.
 36. Grabchev, I.; Bojinov, V.; Moneva, I. *J. Mol. Str.* **1998**, 471, 19.
 37. Proskuryakova, N.; Nurmuknametov, R. *Optics and Spectroscopy* **1969**, 27, 119.
 38. Bhujle, V.; Radhye, M. *Indian J. Chem.* **1971**, 9, 1405.
 39. Koksai, H.; Tumer, M.; Seria, S. *Synth. React. Inorg. Met.-Org. Chem.* **1996**, 26, 1577.
 40. Mohamed, G. G. *Spectrochim. Acta Part A* **2001**, 57, 411.
 41. Kalsi, P. S. *Spectroscopy of Organic Compounds*; 4th ed; New Age International Ltd: New Delhi, 1999.
 42. Freeman, E. S.; Carroll, B. J. *Phys. Chem.* **1958**, 62, 394.
 43. Sestak, J.; Satava, V.; Wendlandt, W.W. *Thermochim. Acta* **1973**, 7, 333.
 44. Coats, A.W.; Redfern, J. P. *Nature* **1964**, 201, 68.
 45. Ozawa, T. *Bull. Chem. Soc. Jpn.* **1965**, 38, 1881.
 46. Wendlandt, W.W. *Thermal Methods of Analysis*; Wiley: New York, 1974.
 47. Horowitz, H.W.; Metzger, G. *Anal. Chem.* **1963**, 35, 1464.
 48. Flynn, J. H.; Wall, L. A. *Polym. Lett.* **1966**, 4, 323.
 49. Kofstad, P. *Nature* **1957**, 179, 1362.
 50. Flynn, J. H. F.; Wall, L. A. *J. Res. Natl. Bur. Stand. A* **1996**, 70, 487.